

Original article

DAMAGE BLOCKS GRANITE OF PHILIP ARRHIDAEUS COMPARTMENT
AND ITS SOURCE AND TREATMENT, KARNAK, EGYPT

Abd-Elkareem, E.¹, Asran, M.² & El Shater, A.²

¹Conservation dept., Faculty of Archaeology, South Valley Univ., Qena, Egypt.

²Geology dept., Faculty of Sciences, Sohag Univ., Sohag, Egypt.

E-mail: elashmawyabdelkareem@yahoo.com

Received 4/2/2017

Accepted 10/7/2017

Abstract

The compartment of Philip Arrhidaeus is one of the most significant Roman landmarks in Karnak Temple. It is exposed to various damage factors. For example, ground water is rising in the study area, causing serious damage to granite used in the compartment. Granite was variously used in Ancient Egypt, both in statues and obelisks. Samples were collected to study their mineral and chemical composition using polarized microscopy, X-ray diffraction, X-ray fluorescence, and scanning electron microscope. Finally, results showed the source of granite, mechanical damage, and the proposed treatment.

Keywords: Granite, Decay, Philip Arrhidaeus compartment, Treatment.

1. Introduction

Karnak Temple dates back to the third family, an archaeological evidence shows that the site has been used since the era of the Middle Kingdom until that of the Romans. It contains many complex buildings that belong to various periods. Ancient Egyptians, like all ancient societies, reused raw materials, especially the construction ones for religious or economic reasons. They used to re-use the building materials, particularly precious ones in private buildings from their predecessors to legitimize new facilities or for economic or political reasons, where restored buildings were destroyed in the era of Akhenaten [1]. Also, many of the Ptolemaic kings renovated many patterns and constructed new buildings close to the Egyptian people [2]. For more than 1,500 years, the Temple of Amun-Ra at Karnak experienced stages of construction, destruction, renewal and expansion [3]. Ptolemaic kings built many

prominent temples in Egypt, e.g. Edfu, Dandara, and Philae in Egypt's informal style with some additions. Moreover, some additions were made to ancient Egyptian temples, such as the Holy of Holies, built by Philip Arrhidaeus [4]. The compartment of the Holy of Holies in Karnak Temple was established by Philip Arrhidaeus (C.356-317). Potentially, Philip Arrhidaeus ordered the construction of the compartment in the place of an old compartment dating back to the reign of Thutmose III. It contained two rooms in the shape of a rectangle; the length of the first was 6 meters and the second was 8 meters. They covered the most important religious scenes on the south wall (right) and those of the coronation of the King, worshipping God, and Amun's sacred boat procession. Landscapes' colors have not changed. Egyptian granite is classified as follows: 1) Older granite, constituting

about 27 % of the Eastern desert Precambrian rocks, covers the composition spectrum of tonrdhjemite, tonalite, granodiorite and rare granite [5], known as grey granite [6]. 2) Younger granite constitutes about 16 % of the Eastern desert Precambrian rocks and comprises late to post-orogenic pink and red granite that ranges in composition from calc-alkaline to alkaline. It is classified into three phases; I, II and, III [7]. Several studies were conducted on Aswan granite due to its importance as an antique building stone [8]. It is called monumental granite in Aswan, and represents large-scale tectonic processes that occurred along the contact between the Arabian Nubian Shield and the Saharan Metacraton [9]. Gindy and Tamish (1998) [10] identified four types of post-collisional, largely undeformed, granites occurred in Aswan area: **a)** Coarse-grained, porphyritic, and fairly mafic “granodiorite”; **b)** Famous coarse-grained, pink to red, and porphyritic monumental granite with rapakivi texture in places; **c)** Fine-grained, mostly pink granite;

and **d)** High-Dam Granite, which is a coarse-grained, mostly non-porphyritic biotite granite. Finger et al. (2008) [11] used the term Aswan Tonalite instead of granodiorite. They added that tonalitic gneiss with a volcanic arc type geochemical signature gave a zircon age of 622_11 Ma, while the Aswan Tonalite and the monumental granite intruded at 606_1 and 606_2 Ma, respectively. High-Dam granite dates back to 595_11 Ma. The regional distribution of these granitoids is shown in fig. (1). Contact relationships indicate that Aswan Tonalite is the oldest intrusion. Monumental granite and fine-grained Saluja-Sehel granite was then intruded [10]. These three form a composite pluton to the south of Aswan. High-Dam granite is the youngest intrusion [10]. It is the largest body and it is located to the farthest south with prominent outcrops near “High-Dam” of the Nile reservoir. This article is concerned with the archaeological history of granite blocks of Philip Arrhidaeus compartment and its quarries.

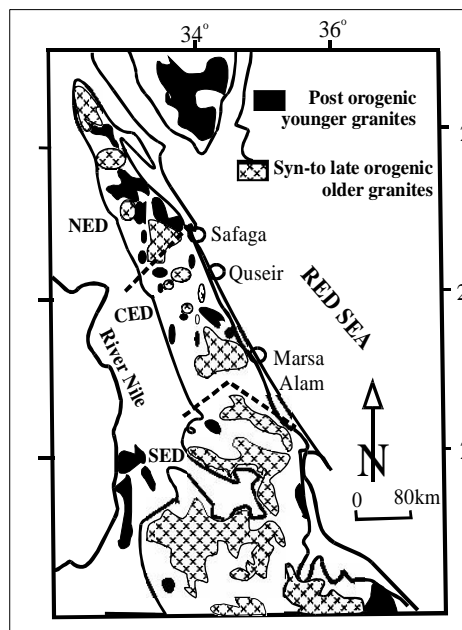


Figure (1) Shows distribution of Egyptian older and younger granites (Modified from the Geological map of Egypt, 1981).

1.1. Field observations and degradation causes

Many ancient quarries were used in ancient Egypt in many constructions [12]. Some scientists report that water in any state physics is the greatest cause of damage processes [13-15]. The granitic

rocks are more responsive to the action of biological activity, air pollution [16], and water where potassium feldspars are converted to kaolinite, with the production of potassium ions, silica and iron

where the latter produces rust [17, 18]. The main weathering forms in Philip Arrhidaeus compartment are exfoliation, granular disintegration, scales, plates, and efflorescence [19, 21], fig. (2-a, b,

c) The disintegration of granules in the granites is attributed to the difference in thermal conductivity of the minerals in the surface layer [22, 23].

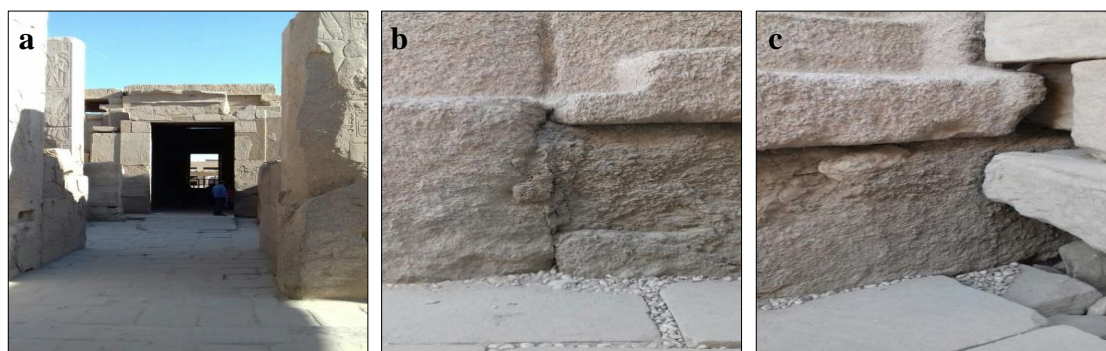


Figure (2) Shows **a**, the entrance of Philip Arrhidaeus compartment, where pitting, grains losing and exfoliation of two sides, **b**, Disintegration of granite surface, **c**, exfoliation and granular disintegration.

1.2. Geology and hydrogeology of the study area

The study area lies within the sedimentary rocks that belong to the Upper Cretaceous era, tertiary, and quaternary. It is a part of complex hydrological systems that dominate the Nile Valley in Upper Egypt, which include many of the aquifers, such as Paleogene, quaternary,

pre-Cenomanian, and Pliocene aquifers [24]. Its southern part is overlain by Nubian sandstone which belongs to the Upper Cretaceous age [25]. Geomorphologically, the site is characterized by hydrographic basins, alluvial plain, structural plains, and river course [26].

2. Materials and Methods

To define the source of the granitic quarry, the authors collected some granitic samples by using non-destructive from Philip Arrhidaeus compartment. These samples were petrographically studied using the polarizing microscope and were chemically analyzed by XRF techniques. Moreover, representative granite samples were powdered and x-rayed to identify, quantify, and characterize their mineral species. The mineralogical analyses were carried out by conventional procedures using X-ray diffraction (XRD) technique.

XRD patterns of powdered bulk samples were recorded using a Philips X-ray diffraction equipment model PW/1710 with monochromator, Cu k - α radiation ($\lambda=1.54 \text{ \AA}$) at 40 kV, 35 mA, in the Department of Physics, Assiut Univ., Egypt. After that, diffraction data were analyzed following El-Shater (2013) [27]. Finally, Scanning Electron Microscope (SEM) was used to study the micro texture, degradation, and deterioration characters of the studied granites.

3. Results

3.1. Petrography

These rocks are pink, coarse-grained, and massive. A thin section shows that the rocks are composed of quartz, feldspars (microcline, microcline perthite, and plagioclase), and biotite. Zircon, sphene, and opaque are accessories. The secondary minerals are represented by

sericite, chlorite, calcite, and epidote. They are characterized by hypidiomorphic texture, fig. (3-a). Alkali feldspars are represented by microcline perthite and orthoclase perthite. Microcline perthite is characterized by vein, patchy, and flame perthite type. Microcline is characterized

by dense crosshatching twinning, fig. (3-b) and including quartz crystals. Orthoclase perthite occurs as subhedral tabular crystals, slightly kaolinitized and displays flame perthite type. Quartz occurs as anhedral coarse crystals showing wavy and undulose extinction. It encloses feldspars, mafic, opaque, and apatite, fig. (3-c). Plagioclase is represented by oligoclase forming subhedral prismatic elongated crystals, characterized by albite twinning and slightly kaolinitized and sericiteized. Some plagioclase crystals are enclosed within microcline and display oscillatory zoned with altered core and fresh rim, fig. (3-d). Mafics are

represented by biotite and arfvedsonite. Biotite occurs as subhedral to anhedral flakes, up to 1.3 mm long, strongly pleochroic, and pale yellow to dark brown, fig. (3-e). Biotite commonly encloses tiny zircon, fig. (3-f). Arfvedsonite occurs as anhedral crystal of dark green colour and strongly pleochroic from green to dark green. It commonly encloses small opaque crystals and sometimes zircon. Opaques occur as isolated grains in different shapes and some of them are perforated by quartz grains.

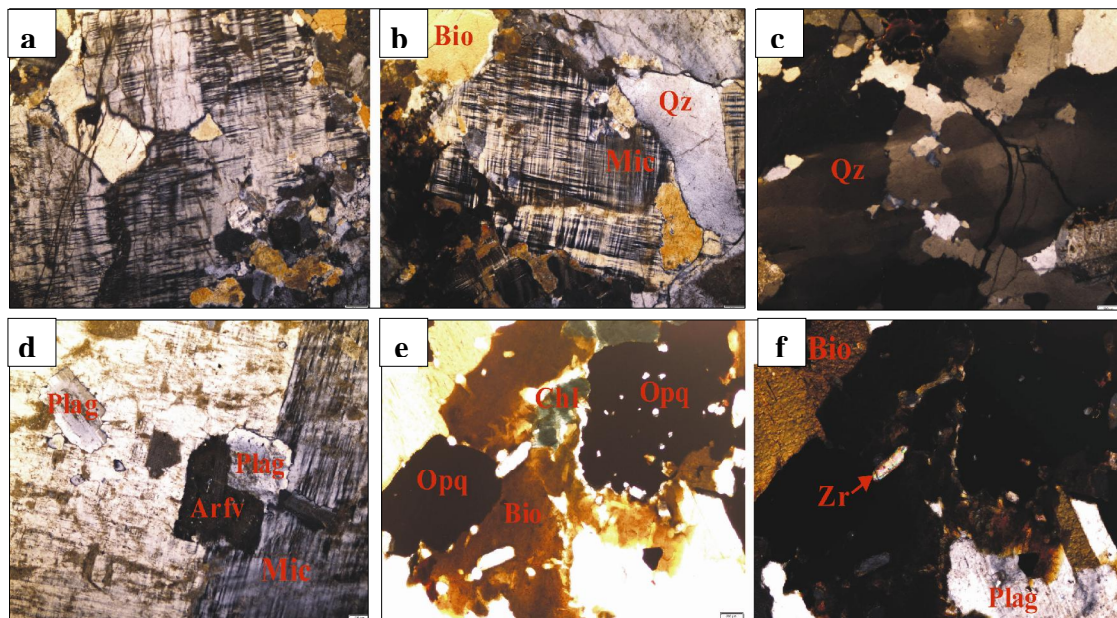


Figure (3) Shows **a**. Hypidiomorphic texture in granite, **b**. Microcline perthite (Mic), **c**. Deformed quartz crystals, **d**. Plagioclase crystals (Plag) and arfvedsonite (Arfv) enclosed by microcline perthite, **e**. opaques perforated by quartz of light colour, Chlorite (Chl) of green colour and Biotite (Bio), **f**. Zircon (Zr) enclosed by biotite in extinction position

3.2. Scanning electron microscope (SEM)

SEM results indicate that the investigated granite samples were highly affected through many deterioration forms these forms such as gaps, grains degra-

dation, presence of some salt species and clay minerals in addition, micro fissures were noticed, fig. (4-a, b).

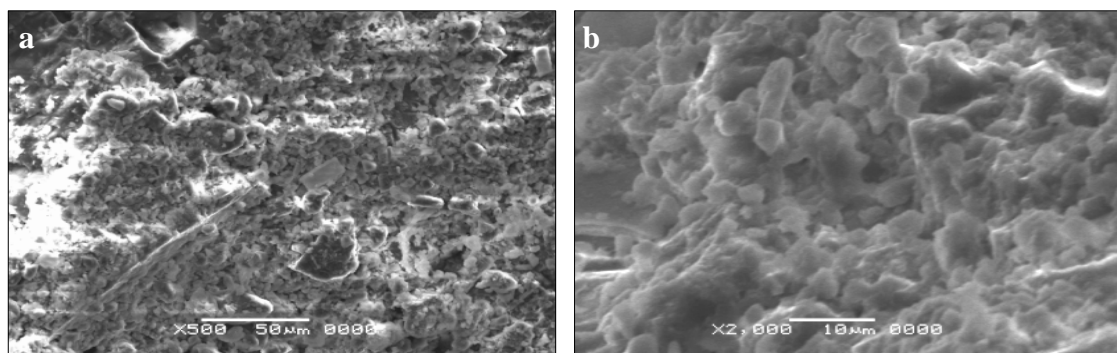


Figure (4-a, b) Shows SEM photomicrographs displaying damage features in the crystals of granite

3.3. Geochemistry

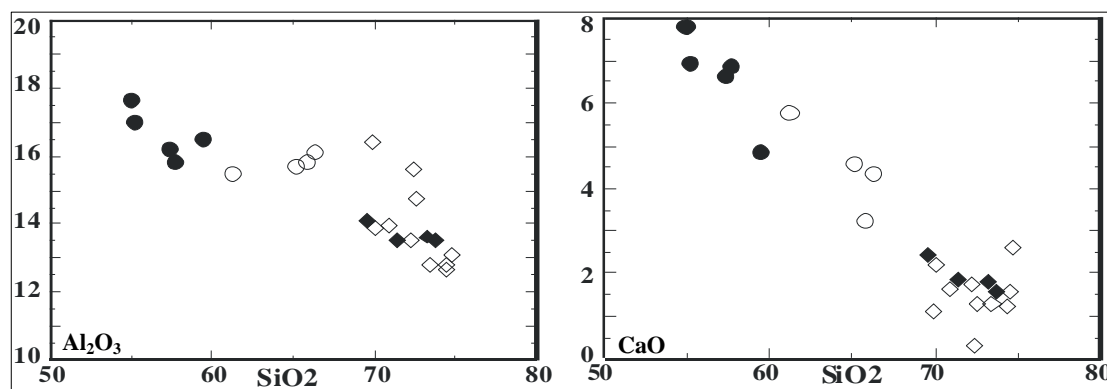
To deduce granite rocks of Philip Arrhidaeus compartment, the authors collected eight samples from Aswan granitoid rocks area [11]. Granite sample from Philip Arrhidaeus compartment were analyzed and listed in tab. (1). Therefore, the authors constructed Harker variation diagrams for some and trace elements versus SiO₂. From the plotted samples, the following could be observed: 1) from most major oxides (i.e., Al₂O₃, MgO, CaO, Fe₂O₃, TiO₂, Na₂O and K₂O) versus SiO₂, the analyzed granite samples are close to the monumental Aswan granite, fig. (5-a). 2) the same feature is re-confirmed by plotting Zr, Y, Ni, Zn, Ga, and Sr versus

SiO₂, fig. (5-b). On the (Na₂O + K₂O) versus SiO₂ (TAS) diagram, fig. (5-c) [28], the analyzed granite samples fall within the granite field and are close to the monumental Aswan granite. Aswan granitoid rocks and the analyzed granite sample from Philip Arrhidaeus compartment are plotted on the A/CNK versus SiO₂. Hence, it is indicated that the granite under study is of metaluminous type (i.e., A/CNK ratio < 1) and similar to the monumental Aswan granite, fig. (5-c). Moreover, the analyzed sample can be described as high-K, fig. (5-c) [29] and similar to mon-umental Aswan granite.

Table (1) Geochemical analyses for the granitoid rocks from Aswan and the granite under study

Sample	1	2	3	4	5	6	7	8	9
Major oxides (wt %)									
SiO ₂	70.48	71.80	58.93	63.50	72.58	68.50	52.49	53.00	72.18
TiO ₂	0.52	0.60	2.11	1.23	0.25	0.50	1.80	2.12	0.39
Al ₂ O ₃	12.80	13.59	12.40	13.50	14.16	15.20	10.83	11.40	12.33
Fe ₂ O ₃	3.32	3.20	10.09	7.47	1.40	2.09	10.20	12.01	3.11
MnO	0.06	0.04	0.16	0.15	0.04	0.06	0.14	0.14	0.05
MgO	0.61	0.40	2.35	1.33	0.31	0.49	5.80	4.42	0.60
CaO	2.26	1.70	5.81	4.00	1.05	1.81	9.25	9.77	1.32
Na ₂ O	3.21	3.35	3.07	3.37	3.32	3.75	2.16	2.39	3.80
K ₂ O	4.75	4.90	1.97	3.17	5.14	5.65	2.51	1.11	4.46
P ₂ O ₅	0.27	0.20	1.04	0.57	0.07	0.15	0.28	0.25	0.16
LOI	1.31	0.71	1.49	0.86	1.39	0.97	3.90	2.90	1.00
Total	99.59	100.49	99.42	99.15	99.71	99.17	99.36	99.51	
A=CNK	0.88	0.98	0.70	0.83	1.09	0.98	0.47	0.50	
Trace elements (ppm)									
Zr	386	335	585	911	190	355	165	175	500
Y	43	20	54	60	27	34	25	31	40
Ga	20	21	23	23	19	21	18	17	20
Ni	6	6	18	13	3	4	43	57	80
Cu	20	18	35	39	14	19	23	18	30
Zn	75	61	162	159	33	66	85	132	10
Sr	211	185	493	357	122	467	245	273	190

1 & 2= Monumental granite, 3 & 4= Aswan Tonalite, 5= Saluja-Sehel granite, 6= High-Dam granite, 7 & 8=Tonalitic gneiss (from Finger et al., 2008). 9= granite under study.



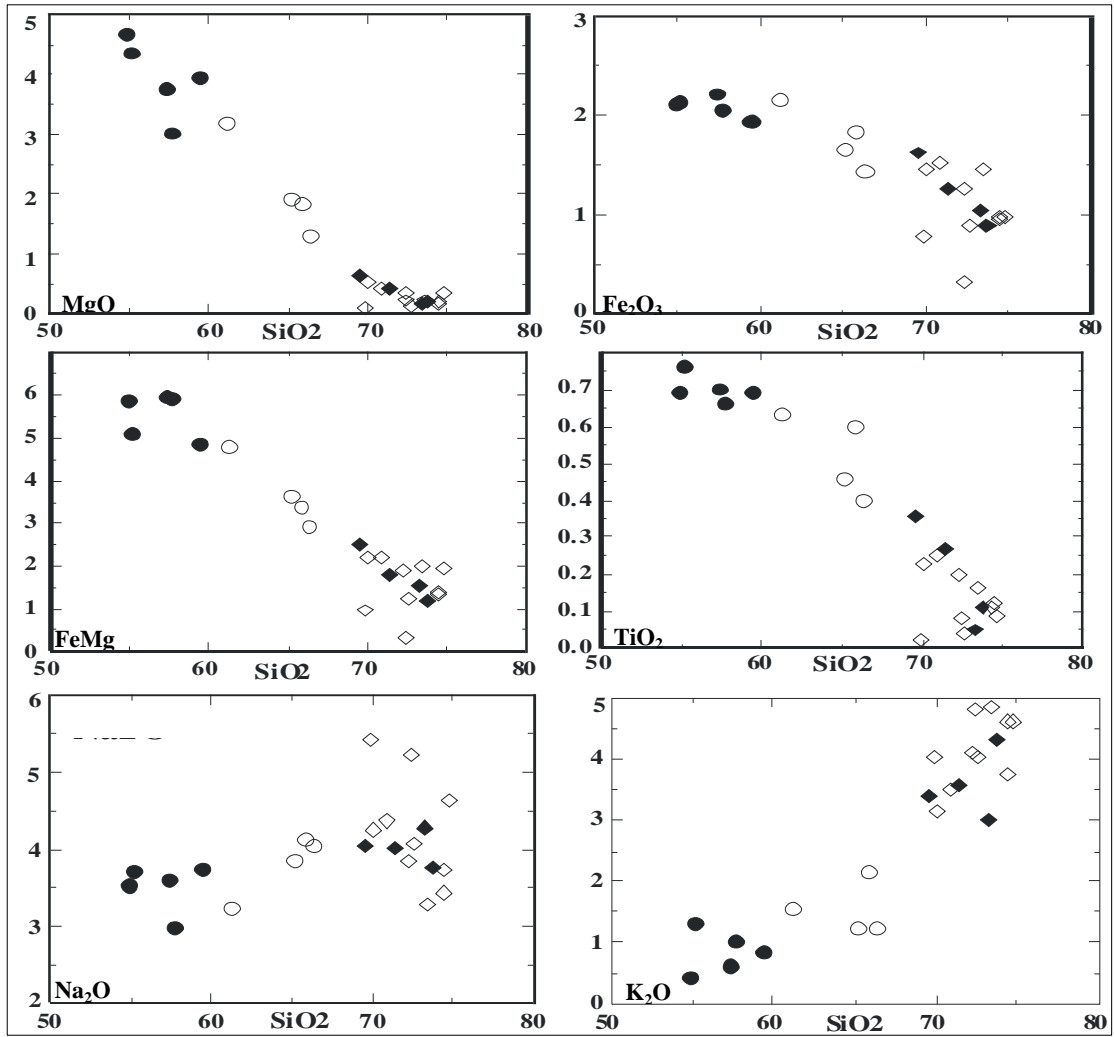
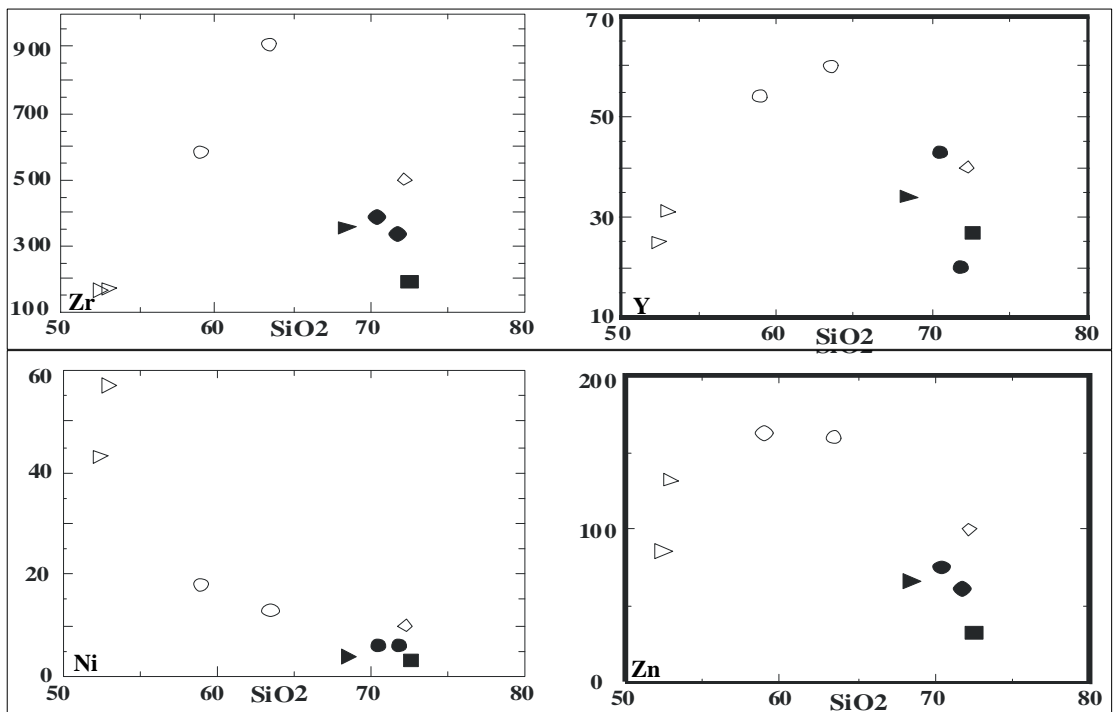


Figure (5-a) Shows variation plot of major oxides versus SiO₂. symbols as follow: (Diorite ●), (Tonalite ○), (Granodiorite ◆), (Granite ◇).



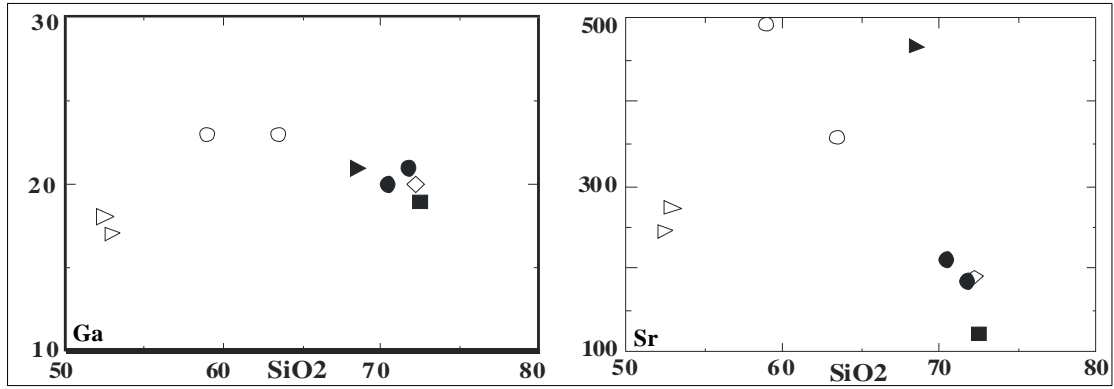


Figure (5-b) Shows variation plot of some trace elements versus SiO_2 for the studied granite and the other Aswan granite.

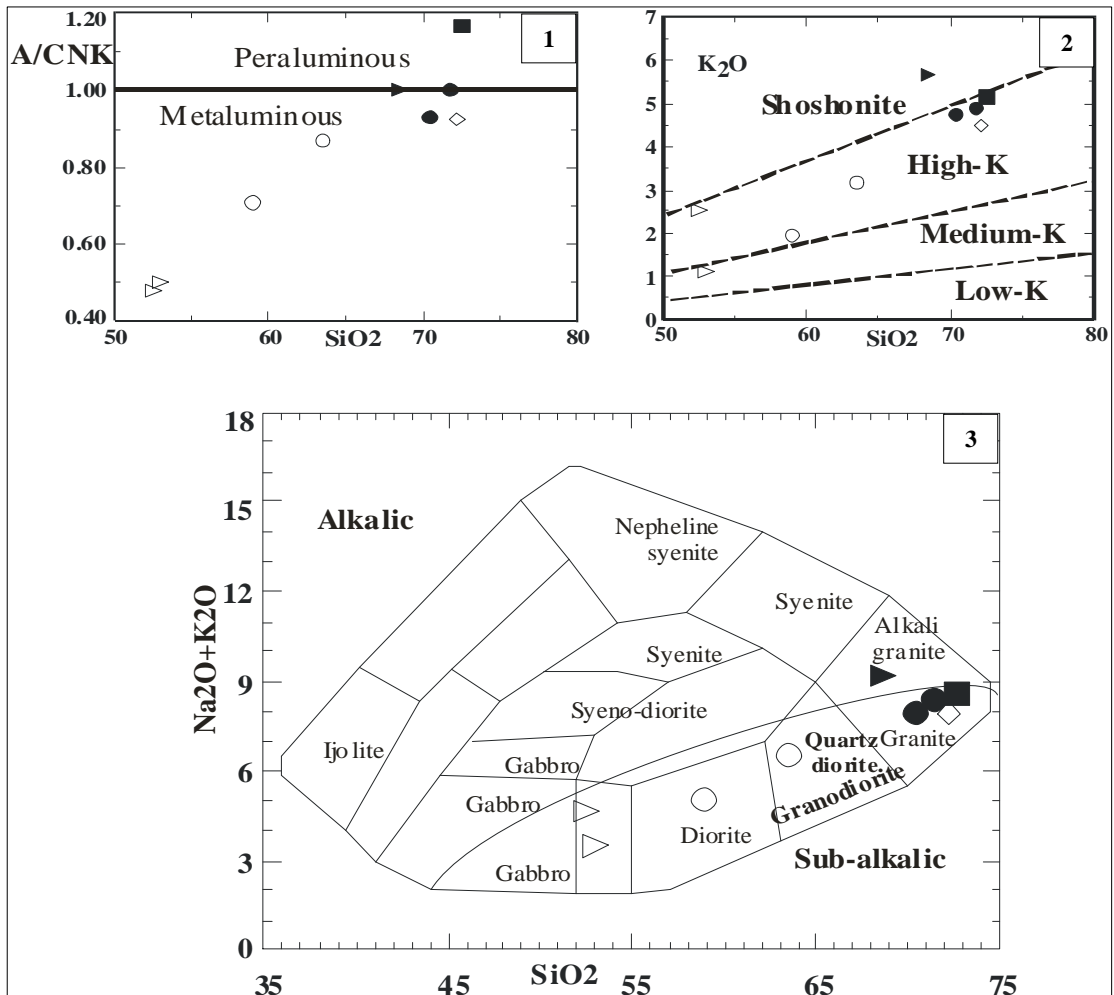


Figure (5-c) Shows **1.** A/CNK vs. SiO_2 , **2.** K_2O vs. SiO_2 (Pecerillo and Taylor, 1976), **3.** TAS diagram for the studied rocks and Aswan granite (Wilson, 1989) The dividing line is from [30] Symbols as in figure 5.

3.4.-XRD analysis of granite bulk samples:

The x-ray diffraction analysis of the powdered bulk samples reveals that the mineral composition of these granites was dominated by feldspar (microcline (53 %); albite (16 %), and anorthite (1 %)), quartz (10 %), mica (muscovite (5 %),

phlogopite (4 %) and biotite (0.4 %), fig. (6-a, b). The morphology of d-spacing of (001) reflections of the main mineral species constituting the studied samples gives conclusive information about the degree of crystallinity of the samples under study,

especially about the stacking defaults along the c-axis. The method of Scherrer uses a single X-Ray reflection for the calculations of mosaic size, but it provides no information on the 'strain' (ϵ), since this affects the profile differently in each 2θ value. The crystallite thicknesses of the

studied profiles of mica range from 16 to 21 nm, quartz from 16-17 nm, albite from 10-11nm, fig. (6-c, d, e). Additionally, following the Williamson-Hall method, the highest strains (0.981) were recorded in the mica crystallites, fig. (6-f), contrary to those of the quartz (0.046), fig. (6-g).

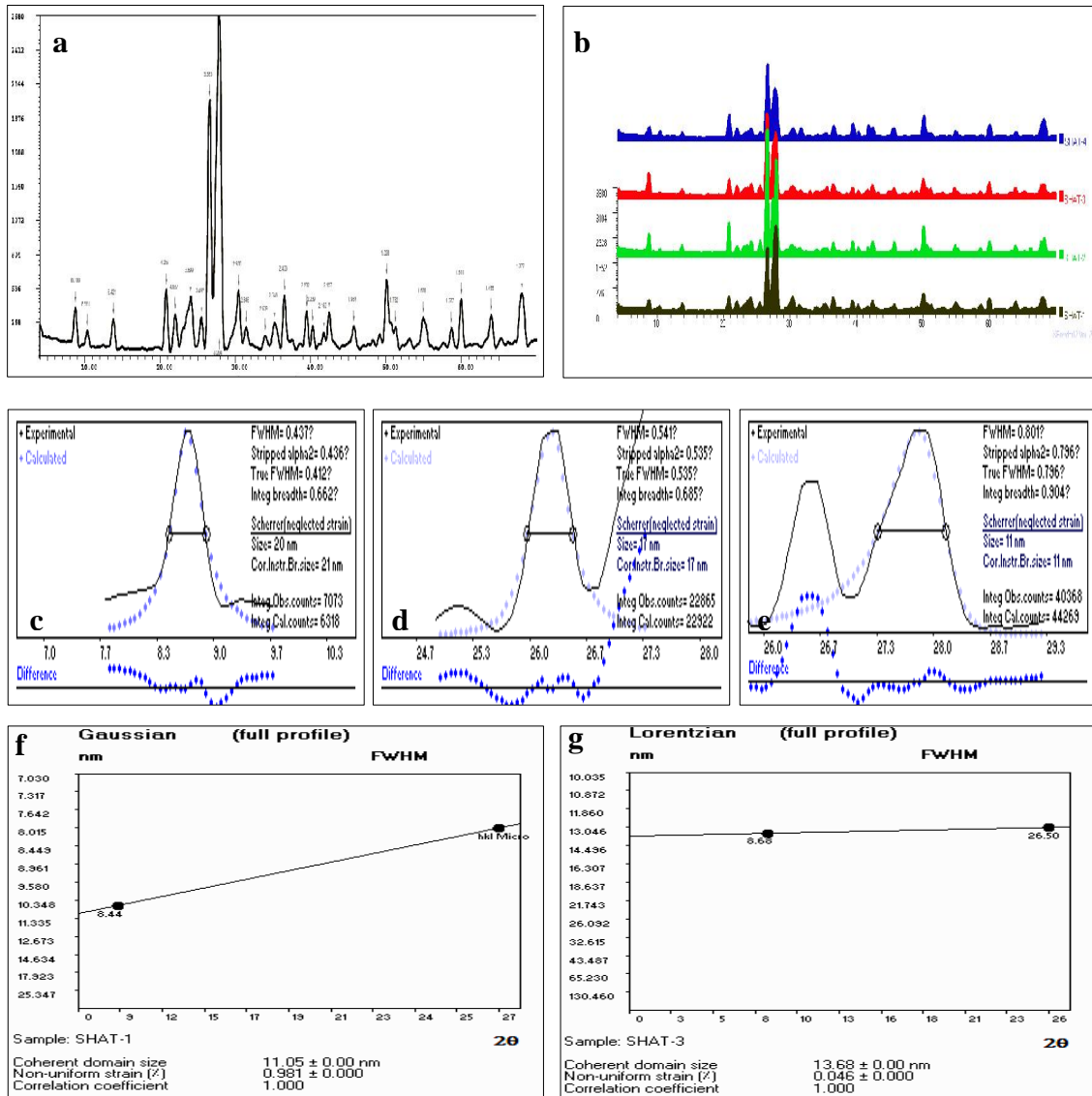


Figure (6) Shows **a**. representative XRD pattern showing the d-spacings identifying the mineral species forming the studied granites, **b**. XRD patterns showing the similarity of the mineral composition of granite under study, **c**. crystallite thickness equation of the muscovite, **d**. of the quartz, **e**. of the albite in the study granitic samples calculated by scherrer, **f**. Non-uniform strain of muscovite of granite under study, **g**. Non-uniform strain of quartz of granite under study calculated by the Williamson-Hall method.

4. Discussion

The study area lies within sedimentary rocks that belong to the Upper Cretaceous, tertiary and quaternary periods. Its southern part belongs to the Upper

Cretaceous Nubian sandstone. Geomorphologically, the area includes hydrographic basins, alluvial plain, structural plains, and river course. It is part of complex

hydrological systems that dominate the Nile Valley in Upper Egypt, including many aquifers, such as: Paleogene, quaternary, pre-cenomanian, and Pliocene aquifers. They represent changes in the climatic factors that cause the damage of granite. While monthly changes in air temperatures in the study area are (14.7 and 32.4 °C), the average monthly relative humidity is (13.0 and 53.0%). Wind speed reaches a monthly average of 2.6 to 17.0 Km/hr. Rains are rare, with a monthly average of 0.0 to 0. mm, according to the 2015. Evaporation varies with time and

place, with a monthly average of 4.7 to 27.3 mm. Accordingly, many changes occurred on the surface of granite and cracks. For example, gypsum and halite crystallized, resulting in salts that attack granite causing different micro cracks. Finally, granite is damaged. The collected samples were examined using X-ray diffraction, polarizing microscope, XRF and SEM. They show a fracture in the inner edges of the grains that may be a result of mechanical damage, fig. (4. a, b).

5. Recommendations

The best solution to the problems of granite damage in the study area is to reduce ground water levels. This can be done by drilling wells around the study area after studying their direction, quantity, and validity. It should also be noted that water is pumped from wells till preventing the withdrawal of the clay because it causes weakness and failure of the bearing soil, resulting in partial or total collapse of the building. Additionally, irrigation network and agricultural drainage should be devel-

oped and Nitrogen fertilizer should be avoided. In addition, sewerage network should be improved and the levels of their lines should be re-examined to make sure that there are no leaks. Furthermore, modern consolidation materials that have been previously used in the consolidation of granite exposed to the damage, due to ground water, sewage or fluctuation of temperatures could be used; the most suitable of which are (MTMOS).

6. Conclusion

*It could be concluded that: 1) The collected sample from the compartment of Philip Arrhidæusis composed of granite which is mineralogically similar to that of Aswan. 2) The geochemical investigations indicate that: * On the TAS diagram, the studied sample is of granite composition which runs in harmony with the petrographic description. * The Harker variation diagrams for the major and trace elements show that the compartment of Philip Arrhidæusis is similar to the monumental Aswan granite. * On the A/CNK and K₂O versus SiO₂ diagrams, compartment of Philip Arrhidæus granite can be said to meet aluminous (A/CNK<1) and as high-K type which is very similar to the monumental Aswan granite.*

References

- [1] Brand, P., (2010). Reuse and restoration, *UCLA Encyclopedia of Egyptology*, Vol. 1 (1), pp: 1-16.
- [2] Sullivan, E., (2008). Architectural features, Digital Karnak, <https://www.scribd.com/document/282153381/karnak-temple-pdf> (10/4/2017)
- [3] Sullivan, E., (2010). Karnak development of the temple of Amun Ra', *UCLA Encyclopedia of Egyptology*, Vol. 1 (1), pp: 1-36.
- [4] Bard, K., (2007). *Introduction to the archaeology of ancient Egypt*, 2nd ed. Wiley-Blackwell, Oxford.
- [5] Hassan, M. & Hashad, A., (1990). Precambrian of Egypt, in: Said, R., (ed.) *The Geology of Egypt*, Balkema, Rotterdam, pp: 201-245
- [6] Akaad, M. & El-Ramly, M., (1960). Geological history and classification of the basement rocks in the central eastern desert of Egypt, *Geol. Surv. Egypt*, Vol. 9, pp: 1-14.

- [7] Akaad, M., Noweir, A. & Kotb, H., (1979). Geology and petrochemistry of granite association of the Arabian desert orogenic belt of Egypt between latitudes 25° 35' and 26° 30', *Delta, J. Sci.*, Vol. 3, pp: 107-151.
- [8] Kelany, A., Negem, M., Tohami, A. & Heldal, T., (2009). Granite quarry survey in the Aswan region, Egypt: shedding new light on ancient quarrying, in Abu-Jaber, N., Bloxam, E., Degryse, P. & Heldal, T. (eds.) *QuarryScapes: Ancient Stone Quarry Landscapes in the Eastern Mediterranean*, Geological Survey of Norway, Special pub., Vol. 12, pp: 87-98.
- [9] Abdelsalam, M., Liégeois, J-P. & Stern, R., (2002). The Saharan Metacraton. *J. Afr Earth Sci*, Vol. 34 (3-4), pp: 119-136.
- [10] Gindy, A. & Tamish, M., (1998). Petrogenetic revision of the basement rocks in the environs of Aswan, Southern Egypt, *Egypt. J. Geol*, Vol. 42 (1), pp: 1-14.
- [11] Finger, F., Dorr, W., Gerdes, A., Gharib, M. & Dawoud, M., (2008). U-Pb Zircon ages and geochemical data for the monumental granite and other granitoid rocks from Aswan, Egypt: Implications for the geological evolution of the western margin of the Arabian Nubian shield. *Mineral Petrol.*, Vol. 93, pp: 153-183.
- [12] Klemm, D. & Klemm, R., (2001). The building stones of ancient Egypt - a gift of its geology, *African Earth Sciences*, Vol. 33, pp: 631-642.
- [13] Shehata, A., (2006). Study the deterioration of granite statues, Keman Fares Excavations, Fayoum, Egypt. *Journal of Engineering Sciences, Assiut Univ.*, Vol. 34 (1), pp: 283-298.
- [14] Ismaiel, B. & Abdel Moneim, A., (1999). Environmental deterioration of Karnak temples, Luxor, Upper Egypt. *Bull Fac. Eng., Assiut Univ.*, Vol. 27 (1), pp: 273-302.
- [15] Helmi, F., (1985). Deterioration of some granite in Egypt, in: Félix, G. (ed.) *Vth Int. Cong. on Deterioration and Conservation of Stone*, Polytechniques Romandes, Lausanne, pp: 421-426.
- [16] Matias, J. & Alves, C., (2001). Decay patterns of granite stones in Braga Monuments (NW Portugal), in: Lourenço, P. & Roca, P. (eds.), *Historical Constructions, Guimarães*, Univ. of Minho, pp: 363-372.
- [17] El-Gohary, M., (2011). Analytical investigations of disintegrated granite surface from the Un-finished obelisk in Aswan, *ArcheoSciences*, Vol. 35, pp: 29-39.
- [18] Rose, R. & Sil, O., (1992). Alteration of igneous rocks by thermo-mechanical Loads, in: Rodrigues, D., Henriques, F. & Jeremias, F. (eds.) *7th Int. Cong. on Deterioration and Conservation of Stone*, Laboratório Nacional de Engenharia Civil, Lisbon, Vol. 2, pp: 651-657.
- [19] Vazquez P., Alonso F., (2015). Colour and roughness measurements as NDT to evaluate ornamental granite decay, *Procedia Earth and Planetary Science*, Vol. 15 pp: 213-218.
- [20] David M., Luz S. & Rafael F., (2015). Microcracking of granite feldspar during thermal artificial processes, *Periodico di Mineralogia*, Vol. 84 (3A), Special Issue, pp: 519-537.
- [21] El-Gohary, M. & Al-Shorman, A., (2010). The impact of the climatic conditions on the decaying of Jordanian basalt: Exfoliation as a major deterioration symptom, *MAA*, Vol. 10 (1), pp: 143-158.
- [22] Evans, I., (1970). Salt crystallization and rock weathering: A Review, *Rev. Geomorphol. Dyn.*, Vol. 19(4), pp: 153-177.
- [23] Whalley, W., Bouglas, G. & McGreevy, J., (1982). Crack propagation and associate weathering in igneous stones. *Zeitschrift for Geomorphologie, N.F.*, Vol. 26, pp: 33-54.
- [24] Farrag, A., (1982). *Hydrogeological studies on the Quaternary water-bearing sediments in area between Assiut and Aswan*. M.Sc., Geology dept., Faculty of Sciences, Assiut Univ., Egypt.

- [25] Said, R., (1981). *The geological evolution of the River Nile*. Springer, New York
- [26] Abu Al-Izz, M. (1971). *Landforms of Egypt*. American Univ. of Cairo Press, Egypt.
- [27] El Shater, A., (2013). Characterization of soil clay minerals of the River Nile sediments, Sohag region, Egypt: Decomposition of X-ray diffraction patterns. *Earth Science and Engineering*, pp: 1-13.
- [28] Wilson, M. (1989). *Igneous Petrogenesis*. Unwin Hyman, London.
- [29] Pecerrillo, A. & Taylor, S., (1976). Geochemistry of Eocene Calc-alkaline volcanic rocks from the Kastamonu area, northern Turkey. *Contrib. Mineral. Petrol*, Vol. 58, pp. 63-81.
- [30] Miyashiro, K., (1974). Volcanic rock series in island-arc and active continental margins, *Am. J. Sci.*, Vol. 274, pp. 321-355.